Modes of deformation and failure of polycarbonate

Roger J. Morgan‡ and James E. O'Neal
McDonnell Douglas Research Laboratories, McDonnell Douglas Corporation, St. Louis, Missouri 63166, USA
(Received 12 June 1978; revised 2 October 1978)

Electron and optical microscopy studies of the modes of deformation and failure of polycarbonate are reported. The high toughness of glassy polycarbonate is controlled by the ease of shear-band deformation and the surface craze characteristics. Such crazes form in tension prior to macroscopic necking and cold-drawing and serve as sites for ultimate fracture. The surface craze characteristics and the role they play in the fracture processes are reported as a function of strain-rate (10^{-2}–10^{+2} min^{-1}) from scanning electron microscopy studies of the fracture topographies and edges of polycarbonate specimens fractured in tension at room temperature. The mechanism by which surface crazing in polycarbonate is enhanced by handling is also reported. The surface regions that come into contact with islands of finger-grease are plasticized, and fabrication stresses within these regions relax near T_g at a faster rate than in the unplasticized surroundings. Microcracks which are produced at the boundary between the plasticized and unplasticized regions serve as sites for craze initiation and growth. The craze processes in thin polycarbonate films strained directly in the electron microscope are also reported. Undeformable ~10 nm sized nodular regions were observed during the craze flow processes in these thin films.

INTRODUCTION

Polycarbonate is a tough thermoplastic with good impact properties. This amorphous but crystallizable glass is, however, susceptible to solvent-crazing[1–8] and, also, can embrittle on annealing below T_g[8–23]. To predict the durability of polycarbonate in a service environment with confidence requires a knowledge of (a) the physical arrangement of the macromolecules in the bulk, (b) the microscopic modes of deformation and failure, (c) the structural parameters that control the modes of deformation and failure, (d) the effect of the modes of deformation and failure on the mechanical response and (e) how these interrelations are modified by fabrication procedures, specimen geometry and environmental and stress exposure.

Precrystalline or crystalline structures do not form in bulk polycarbonate below T_g ($T_g \simeq 150°C$)[18,20,23–25]. Indeed, annealing polycarbonate below T_g produces only changes in free volume which are reversible for reversible thermal anneal cycles[18,20,23]. Polycarbonate does, however, crystallize immediately above T_g, which allows precrystalline or crystalline entities to grow below the bulk T_g in thin films and on free surfaces of thick films where mobility restrictions are less severe than in the bulk[18,20,26–31]. The surface structures consist of aggregates of 5–6 nm diameter nodules, which are the size of ordered molecular domains[18–20,23,29]. There is, however, no evidence that similar morphological entities form in the bulk above T_g during the initial stage of crystallization. Although these surface morphological entities do not play a direct role in the bulk flow processes of polycarbonate, such structures could affect the failure initiation processes which generally occur at surfaces.

Polycarbonate is a tough, ductile material which deforms by shear yielding, even at cryogenic temperatures, in the absence of flaws of critical geometries[8]. Surface flaws are, however, often produced during the fabrication of polycarbonate specimens by, for example, machining, drilling or sawing. Also, exposure to organic environments, such as handling, together with interaction with fabrication stresses are sufficient to generate critical surface flaws. Polycarbonate, typical of a ductile thermoplastic, is extremely notch sensitive[22,32]. This glass embrittles as a result of the cessation of shear yielding and reverts to a crazing deformation mode with a corresponding decrease in molecular flow and energy to failure[12,18,20,23,33].

In addition to surface flaw characteristics, the embrittlement of polycarbonate is dependent on specimen thickness, molecular weight, thermal history, strain-rate and test temperature. The mechanical response of a polycarbonate specimen containing a critical flaw is sensitive to specimen thickness as a result of plane-strain conditions in the deformation zone because lateral contraction becomes inhibited with increasing thickness[10,15,17,18,20,21,34–37]. For plane-stress conditions, shear-band deformation is favoured; for plane-strain conditions, crazing and premature fracture is favoured. Indeed, Mills[21] reports that notched polycarbonate bars >5 mm thick are always brittle from $-196°$ to $115°C$ in the impact strain-rate region. Fraser and Ward[38] have found that the fracture toughness of notched polycarbonate specimens depends on molecular weight in addition to the notch-tip radii. They suggest that lower-molecular-weight polycarbonates possess lower crazing stresses and, therefore, exhibit more brittle mechanical responses. For polycarbo-

* Research sponsored in part by the McDonnell Douglas Independent Research and Development Program and in part by the Air Force Office of Scientific Research/AFSC, United States Air Force, under Contract No. F44620-76-C-0075. The United States Government is authorized to reproduce and distribute reprints for governmental purposes notwithstanding any copyright notation hereon.
‡ Present address: Lawrence Livermore Laboratory, L-338, University of California, P. O. Box 808, Livermore, CA 94550

0032–3861/79/030375–13$02.00

nate specimens < 5 mm thick, a transition from ductile to brittle behaviour has been observed with increasing strain-rate and/or decreasing temperature[15,18,20,22,33,34]. This embrittlement is also affected by thermal history because above 80°C, polycarbonate has sufficient molecular mobility to allow decrease in free volume. These liquid-like packing decreases in free volume inhibit molecular flow associated with both shear yielding and crazing and cause the glass to be more sensitive to craze/crack growth[18,20,23].

Hence, the embrittlement and durability of polycarbonate depend on a complex number of interacting phenomena, not all of which are completely understood.

This study addresses three areas related to the modes of deformation and failure of polycarbonate which are pertinent to its embrittlement and durability:

(1) In previous studies we observed a ductile-brittle transition in tension at a strain-rate of $\sim 10^2$/min for 1 mm thick, unnotched polycarbonate specimens that had been annealed at 125°C[18,20,23]. At lower strain-rates and greater free volumes (i.e., quenched or 145°C equilibrium-state glasses), shear-band deformation was the predominant mode of deformation, whereas crazing became the predominant mode on embrittlement at higher strain-rates. Kastelic and Baer[39] have reported that at room temperature and above, crazes form in polycarbonate prior to shear-band deformation and cold-drawing at strain-rates of $\sim 10^{-2}$/min. Such crazes appear to be blunted by micro-shear bands and do not readily nucleate fracture. They also noted that subsequent shear-band formation and propagation is unhindered by the presence of these crazes. In earlier studies on polycarbonate, Spurr and Niegisch[1] also reported that crazes are carried through and survive the necking process virtually unchanged in size or shape. However, more recently Cornes, Smith and Haward[40] reported that such crazes formed at 70°C in polycarbonate develop into diamond-shaped cavities during cold-drawing, and final fracture occurs by the interconnection of adjacent diamond cavities.

In this study scanning electron micrographs of the fracture topographies and edges of 1 mm thick polycarbonate specimens fractured at room temperature as a function of strain-rate from 10^{-2} to 10^{+2}/min were investigated. Such studies reveal how the modes of deformation and failure, including surface crazes, vary with strain-rate. The characteristics of these surface crazes can control directly the stage of deformation at which fracture occurs and, hence, the mechanical response of polycarbonate.

(2) The initiation and propagation of crazes in polycarbonate are enhanced by exposure to certain organic chemicals[1–8]. Polycarbonate crystallization is enhanced by the presence of plasticizers which allow the greater chain mobility necessary for crystallization[2,4,28,29,41–45]. Neki and Geil[29] report that even a fingerprint will cause crystallization on the surface of polycarbonate after annealing at 110°C. Miller *et al.*[2] have suggested that the solvent crazing of polycarbonate is caused by stresses arising from the crystallization process. Certainly surface crystallization can cause sufficiently high surface stresses to produce micro-cracks. We have observed directly surface micro-cracks along the edges of prespherulitic arms on the surface of polycarbonate[16,18]. Kambour[3] notes, however, that solvent crazing behaviour of polycarbonate is too similar to that of non-crystallizable polymers to involve a separate and distinct mechanism dependent on crystallizability. Caird[8] has documented that handling the surface of polycarbonate followed by exposure to 130°C under stress causes crazing and seriously deteriorates the mechanical response relative to untouched glasses exposed to the same temperatures and stresses. In this study we investigated the embrittlement of polycarbonate caused by handling, using optical and scanning electron microscopy to elucidate the primary mechanisms responsible.

(3) Electron microscopy has been used to investigate the microscopic deformation modes of polycarbonate by studying microtomed sections[46–48] or replicas of prestrained films[4,5,27,28,49]. However, we have found polymer films strained directly in the electron microscope can also generate useful information on the modes of deformation of polymers[23,50–52] and, therefore, have conducted similar studies on polycarbonate.

EXPERIMENTAL

Materials and sample preparation

The bisphenol A polycarbonate (poly-4,4′-dioxydiphenyl 2,2-propane carbonate) (Lexan, General Electric Co.) had a viscosity-average molecular weight of 30 000 and contained no significant additives. The polymer in the powdered form and prior to any sample preparation was preheated at 125°C overnight in vacuum to remove moisture.

For the fracture topography specimens, compression-moulded sheets (~1.0 mm thick) of polycarbonate were prepared by moulding the dry polymer powder at 180°C for 15 min at ~35 MPa and then cooling under pressure to room temperature at 2°C/min. Dogbone-shaped specimens, suitable for tensile fracture, were machined from the sheets, and the edges were polished along the gauge length. These specimens were then vacuum annealed at 160°C for 1h, which minimized fabrication stresses, and then annealed below T_g at either 145° or 125°C.

Discs, ~3 cm in diameter and ~1.0 mm thick, to be utilized in the studies of the embrittlement of polycarbonate as a result of handling were prepared in circular moulds under the same conditions as those used for the fracture topography specimens. These specimens, however, were not annealed after moulding.

Polycarbonate films, ~1 μm thick, suitable for straining directly in the electron microscope were prepared by spreading a few drops of a 1% solution of the polymer in methylene chloride onto NaCl crystals. The films and substrates were exposed to vacuum for 12 h at room temperature, and any remaining solvent was evaporated at 160°C for 30 min. under vacuum. The salt crystals were dissolved in water, and the films were washed with distilled water. Specimens, 2 mm square, were cut from the polycarbonate films.

Experimental

For the fracture topography studies, the dogbone-shaped samples were fractured in tension at room temperature in a tensile tester (Instron TM-S-1130) at crosshead speeds of 0.05 to 100 cm/min. A scanning reflection electron microscope (Jeol model JEM-100B) was used to study the fracture topographies and edges of these specimens. For these studies the fracture surfaces and edges were coated with gold while the sample was rotated in vacuum.

To study the effects of handling on the embrittlement of polycarbonate, a single thumbprint was placed on the surface of the polycarbonate disc. This disc was then stressed at ~10 MPa (at its maximum cross-section) for 1h at 130°C. The disc was then examined at room temperature by reflection and transmission optical microscopy, using an optical microscope (Zeiss Ultraphot II), and scanning reflection electron microscopy. The disc was coated with gold prior to the scanning electron microscopy studies.

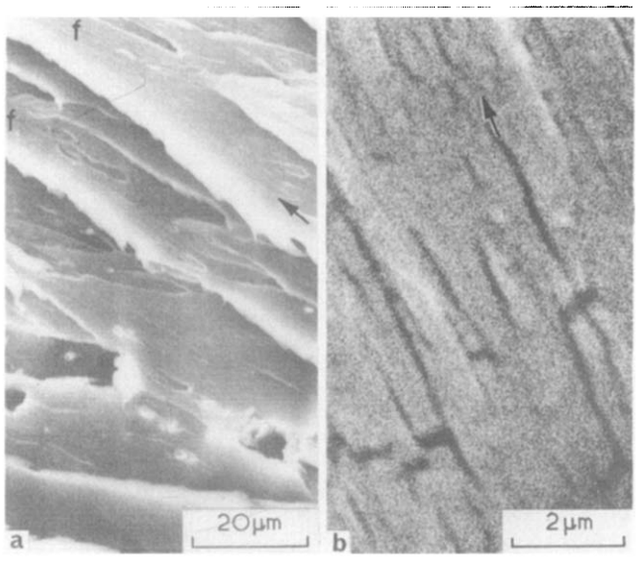

Figure 1 Scanning electron micrographs of fracture surfaces of polycarbonate that deformed and failed under a strain-rate of $\sim 10^{-2}$ min^{-1} illustrating (a) parallel planes that intersect at the flaplike structures (f) and (b) microcracks within these planes (arrows indicate direction of crack propagation).

Bright-field transmission electron microscopy was used to monitor the modes of deformation of the ~1 μm thick films that were strained directly in the electron microscope. The 2 mm square polycarbonate specimens were fastened to standard cartridge specimen holders with cement (Duco E. I. duPont). The specimen holder was attached to an EM-SEH specimen elongation holder which was introduced into the microscope through the side-entry goniometer. The specimens were deformed in the microscope at a strain-rate of $\sim 10^{-2}$ min^{-1}.

RESULTS AND DISCUSSION

Variation of modes of deformation and failure with strain-rate

The fracture topographies and edges of the 1 mm thick polycarbonate specimens fractured at room temperature were monitored as functions of strain-rate from $\sim 10^{-2}$ to 10^{+2} min^{-1}. The fracture topographies and edge features of these specimens were similar for both the 125° and 145°C annealed polycarbonates, with the exception that only the 125°C annealed glasses deformed predominantly by crazing in the $\sim 10^{+2}$ min^{-1} strain-rate region.

In the 10^{-2}–1 min^{-1} strain-rate region, polycarbonate deformed predominantly by macroscopic shear-band deformation, and all specimens exhibited necking and cold-drawing prior to fracture by fast crack propagation through the oriented neck. The fractured specimens decreased in width, thus indicating plane stress fracture conditions. The fracture topographies exhibited striations parallel to the direction of crack propagation[18,21,33,50]. The striations are steps formed by the subdivision of the crack front into segments running on parallel planes as illustrated in *Figure 1a*. A similar subdivision of the crack front produces river markings in the more brittle polymeric thermosets[51,53,54]. The flaplike striations [designated by (f) in *Figure 1a*]that occur at the intersections of the crack planes are a result of tearing and cold-drawing of the polymer and have been observed by Mills[21] for polycarbonate and Murray and Hull[55] for polystyrene. The parallel planes shown in *Figure 1a* exhibit finer striations which are situated parallel or perpendicular to the direction of carck propagation, as illustrated in *Figure 1b*. These finer striations appear to be fine cracks which could result from the relaxation of a surface layer of polymer that has been swept onto the fracture surface and oriented in the direction of crack propagation. Elongated fractured fibrils that have been swept down onto the fracture surface have been reported by Doyle[56,57] and Hoare and Hull[58] for polystyrene and by the authors for epoxies[50,59]. Indeed, in certain areas of the polycarbonate surface we observe 100–200 nm diameter fibrils that have been swept onto the fracture surface and aligned in the direction of crack propagation, as illustrated in *Figure 2*.

Examination of the edges of the polycarbonate specimens that deformed in the 10^{-2}–1 min^{-1} strain-rate region revealed a network of cavities as illustrated in *Figure 3a*. These cavities propagated from surface crazes which had developed prior to cold-drawing and had passed into the necked region. The formation during the cold-drawing process of diamond-shaped cavities that initiate from either crazes or surface defects has been reported for a number of polymers, including polycarbonate[40,60–62]. Such cavities propagate by tearing at the pointed tips of the diamond resulting in a cavity consisting of two straight edges and two pointed extremities[40,60]. The remnants of such cavities are found in *Figures 3a* and *b*. However, many of the surface cavities illustrated in *Figure 3a* are too irregular to be associated with original diamond-shaped structures. Cornes *et al.*[40,60] report that the nature of this plastic deformation is controlled by the presence of four shear bands which propagate from each end of the straight edges of the cavity. These cavities grow to thicknesses that are many times that of the original craze. Fracture of the polycarbonate specimens occurs by interconnection of the cavities illustrated in *Figure 4a*. Cornes, Smith and Haward[40] have noted that fracture by this process is controlled by the stress concentrations associated with the cavities, which depend on the cavity size and tip radii, the stored elastic energy within the specimen, and the strain-hardening characteristics and crack resistance of the oriented polymer. Cornes and

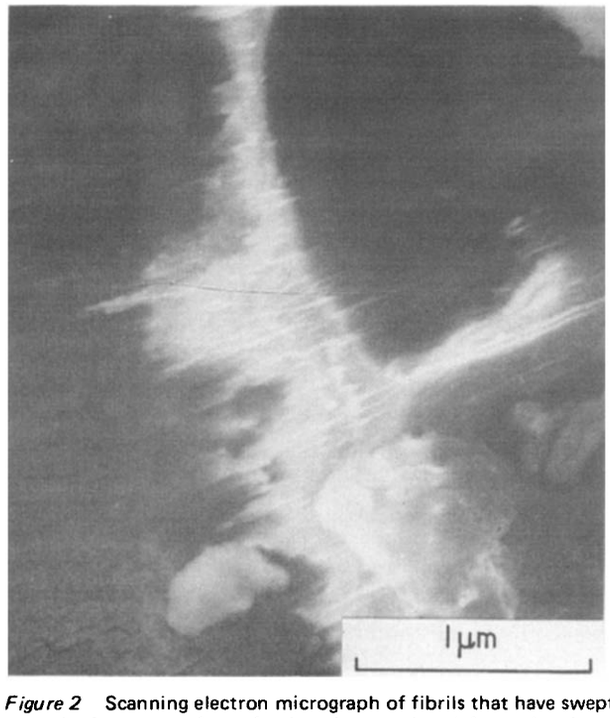

Figure 2 Scanning electron micrograph of fibrils that have swept onto the fracture surface of polycarbonate that deformed and failed under a strain-rate of $\sim 10^{-2}$ min^{-1}

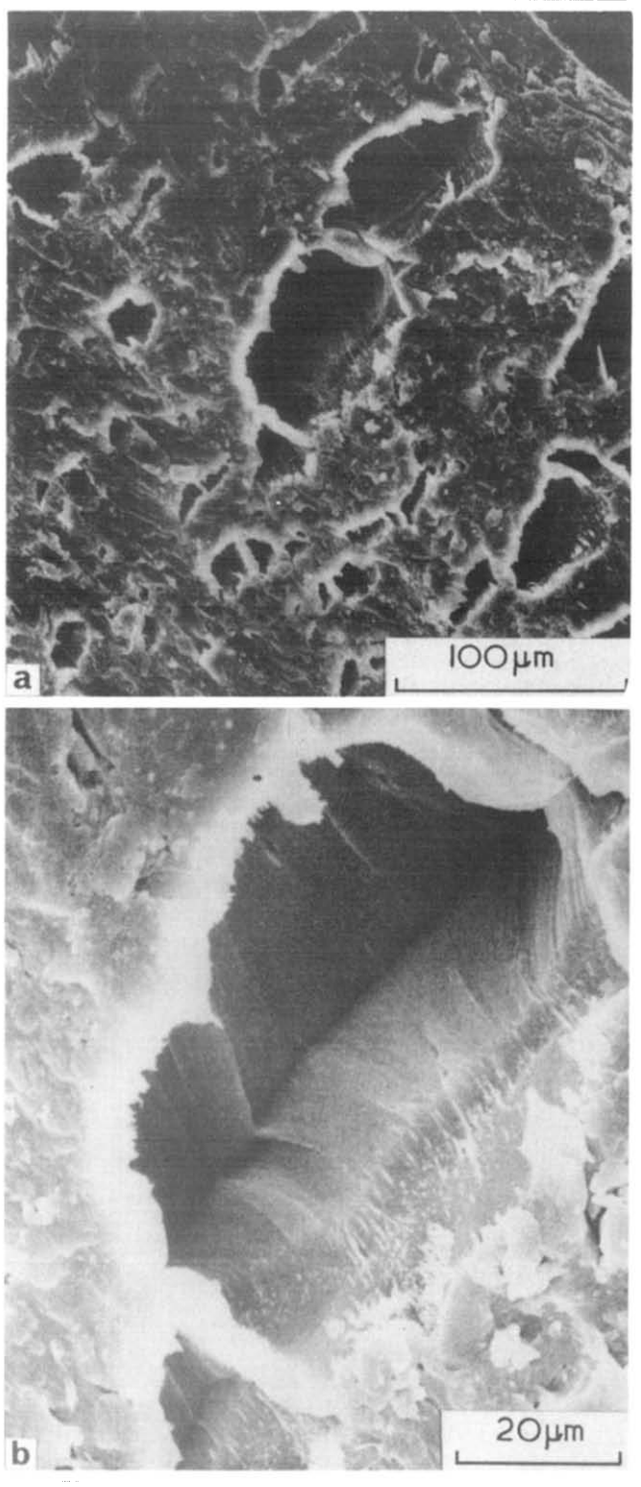

Figure 3 Scanning electron micrographs of the edge of cold drawn polycarbonate that deformed and failed under a strain-rate of $\sim 10^{-2}$ min^{-1} illustrating (a) numerous edge cavities and (b) the topography within a cavity

Haward[60] associate the smoothness of the cavity walls (*Figure 3b*) with a slow tearing process. The fractured fibrils on the cavity walls near the specimen surface in *Figure 3b* originate from the original craze that formed prior to cold-drawing. A distinct boundary is evident in this micrograph between the interior smooth surface associated with the tearing of non-crazed material and the exterior fibrillar, crazed region of the cavity. The latter region has propagated to a depth of 5–10 μm into the specimen prior to the onset of the tearing process.

Hence, polycarbonate specimens that were strained in the 10^{-2}–1 min^{-1} strain-rate region deform predominantly by shear-band deformation and cold-drawing. However, surface crazes that form prior to macroscopic necking and cold-drawing serve as sites for subsequent plastic tearing and ultimate fracture.

In the 1 to 10^{+2} min^{-1} strain-rate region, polycarbonate still deforms predominantly by macroscopic shear yielding and subsequent cold-drawing. The crazes that form prior to the cold-drawing process are, however, $\geqslant 100$ μm in length which is tenfold larger than those that grew in the 10^{-2} to 1 min^{-1} strain-rate region. Such crazes act as sites for crack growth and ultimate failure of the glass.

The fracture topography of an edge craze in the 1 to 10^{+2} min^{-1} strain-rate region is illustrated in *Figure 4* in which a curved, cusp separates the edge craze topography from that of the cold-drawn region. In the regions where the craze was thickest, nearer the specimen edge, a patch pattern in the fracture topography is observed as illustrated in *Figure 5a*. The protruding patches and depressions on one fracture surface match the reverse pattern of protrusions and depressions on the opposite fracture surface. This type of topography is associated with crack propagation along the boundary between the crazed and uncrazed material with the crack jumping irregularly from one boundary to the other[18,33,63,64]. In previous studies the patches, whose thicknesses are those of the original craze, were generally found to be smooth with no fine structure. In this case, however, the protruding patches exhibit a distinct topography of fractured fibrils interdispersed by voids as illustrated in *Figures 5b* and *c*. The depressions on one fracture surface that match the protruding patches on the opposite fracture surface are relatively smooth with the exception of a few fractured fibrils which are perpendicular to the surface (*Figure 5a*). Similarly situated fibrils have been observed by Doyle[56] in the fracture surfaces of preoriented polystyrene. The voids on the protruding patches were largest in the regions associated with the thickest portion of the original craze and exhibited a dimple-like structure with dimple diameters of 1–5μm (*Figure 5b*). (In metallurgy a dimpled fracture topography is associated with a ductile fracture mode that involves nucleation, growth and coalescence of voids by internal necking[65–67].) The dimples in the polycarbonate fracture topography are separated from one another by a single

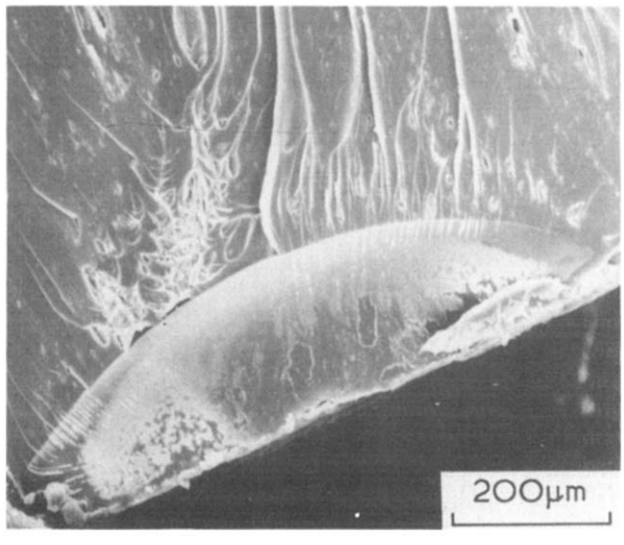

Figure 4 Scanning electron micrograph of the fracture topography of an edge craze in polycarbonate (strain-rate of ~ 2 min^{-1})

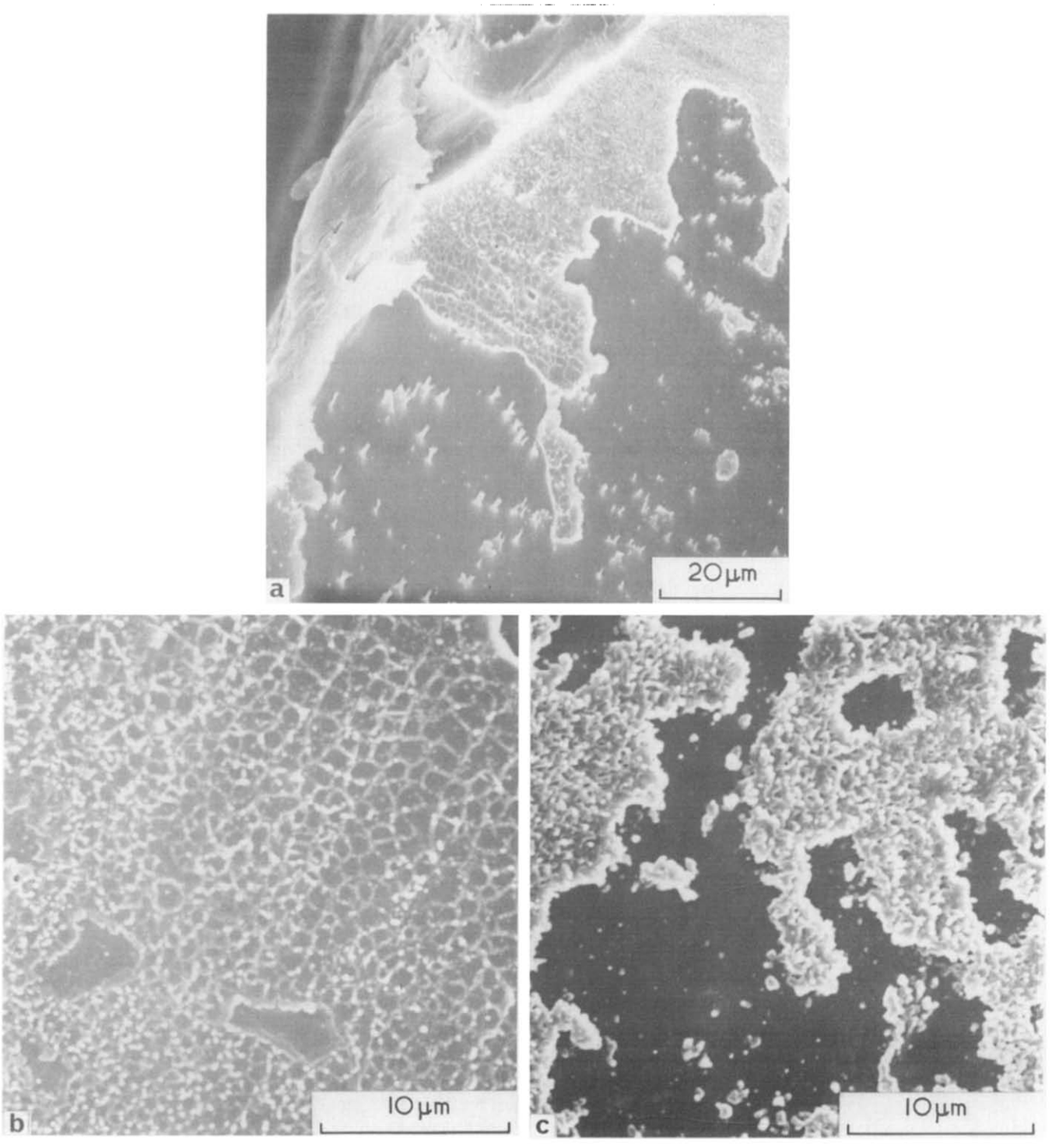

Figure 5 Scanning electron micrographs of the patch-pattern fracture topography of an edge craze in polycarbonate that deformed and failed under a strain-rate of ~2 min^{-1} illustrating (a) overall, (b) dimpled and (c) fibrillar topographies

boundary of fractured fibrils which are ⩽ 500 nm in diameter. The surfaces of the protruding patches develop a more fractured fibrillar appearance as the voids decrease in size with decreasing thickness of the original craze (*Figure 5c*).

The overall fracture topography nearer the tip of the craze is shown in *Figure 6a*. The patch pattern persists in this region, but the patches are much thinner than those nearer the specimen edge because the craze tapers to a thin section. In this region 100–300 nm diameter voids and poorly developed fibrils are evident (*Figures 6b* and *c*). These voids are considerably smaller than those observed in the thicker regions of the original craze. This observation is consistent with other fracture topography studies that also reported a decrease in void size as the craze tip is approached[68,70]. The voids and poorly formed fibrils taper to a series of fine fingers near the craze tip as illustrated in *Figure 6a*. These regions are shown in more detail in *Figure 7*. Highly drawn, thin films of polymer that are perpendicular to the fracture surface and parallel to many of the fine craze fingers are evident in *Figure 6a*. These highly drawn regions are caused by the crack propagating at a slower rate

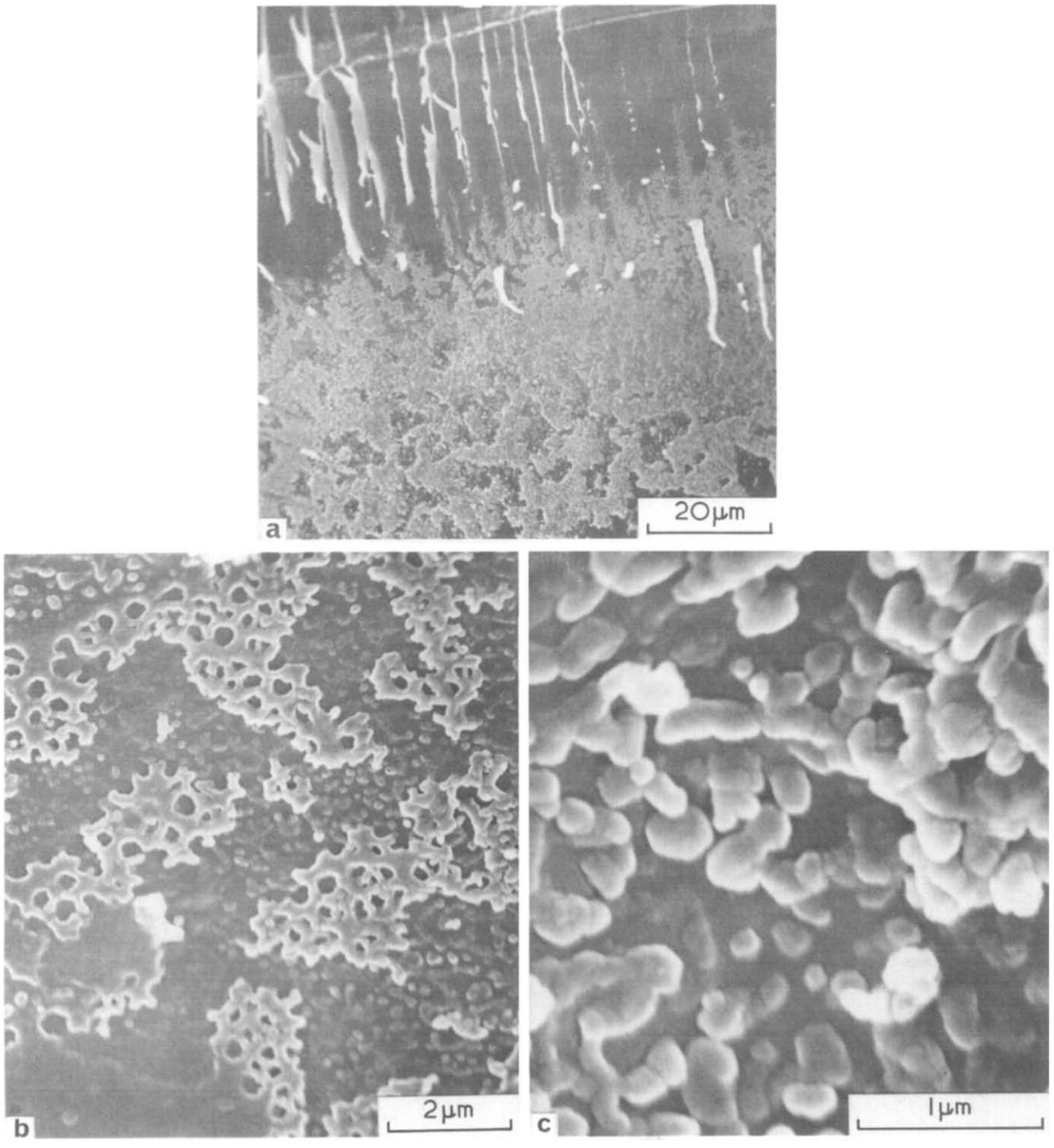

Figure 6 Scanning electron micrographs of craze tip fracture topography of edge craze in polycarbonate that deformed and failed under a strain-rate of ~2 min^{-1} illustrating (a) overall, (b) microvoid and (c) poorly developed fibrillar topographies of this region

through the crazed fingers and thus lagging-behind the general crack front. No evidence of significant ductile tearing of the craze as a result of cold-drawing was found in the fracture topography crack tip region in *Figure 6a*.

Crazes normally grow preferentially by areal growth rather than by a thickening mechanism caused by drawing new material across the craze-matrix boundary interface[3,71]. In the 1 to 10^{+2} min^{-1} strain-rate region, however, after cold-drawing occurs, the oriented material at the craze tip inhibits further areal craze growth in polycarbonate. Crazes do not propagate easily through polymeric material oriented perpendicular to the craze growth direction[72,73]. Also, no significant growth of the craze occurs by the ductile tearing process that was observed at lower strain-rates. Therefore, during cold-drawing the craze extends by further internal void growth, coalescence and fibrillation. The strains produced during cold-drawing will be greatest in the thicker regions of the original craze thereby causing larger voids in these regions because of fibrillar fracture and void coalescence.

The distinct porous-fibrillar structure present on the surfaces of the protruding patches in the thicker craze regions

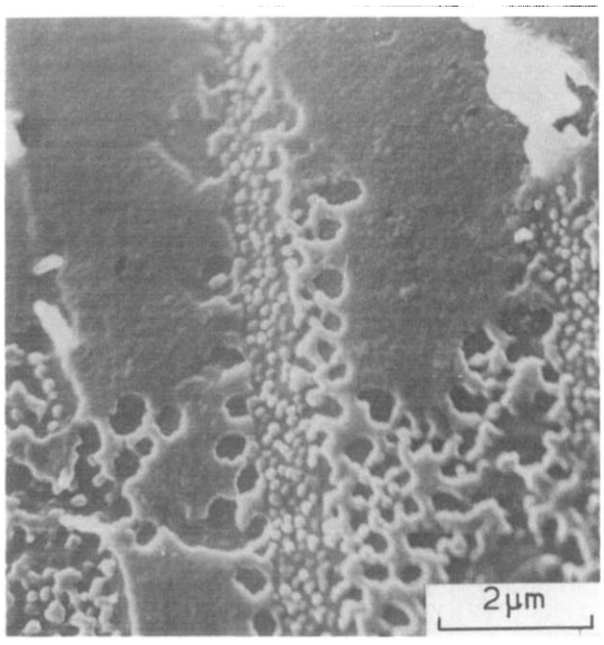

Figure 7 Scanning electron micrograph of fracture topography of craze fingers at tip of edge craze in polycarbonate that deformed and failed under a strain-rate of ~2 min^{-1}

results from crack propagation along the craze-matrix boundary interface. This structure is unusually distinct possibly because of abnormal stresses in the craze, and at the craze-matrix boundary interface during crack propagation caused by the oriented state of the surrounding material. The magnitude and distribution of the stress fields in the vicinity of these crazes during fracture will be different than those that exist in polymers which deform only by crazing.

The fracture topography of the crazes that initiated fracture in polycarbonate in the 1 to 10^{+2} min^{-1} strain-rate region did not exhibit any characteristic slow crack-growth regions on matching fracture surfaces. Initial crack propagation generally proceeds through the median of the craze[51,54,55,57,59,63,74] producing a fractured fibrillar or rough topography on matching surfaces[51,54,59]. The absence of a slow crack-growth region suggests that significant crack growth occurred only under the influence of the highly strained surrounding cold-drawn material rather than prior to the onset of cold-drawing.

Hence at room temperature in 1 to 10^{+2} min^{-1} strain-rate region, polycarbonate still deforms predominantly by shear-band deformation and cold-drawing. However, the surface crazes that form prior to cold-drawing and cause ultimate fracture are tenfold larger than those that form in the 10^{-2} to 1 min^{-1} strain-rate region. Also, significant plastic tearing does not occur from these larger crazes prior to catastrophic crack propagation.

In the 10^{2} min^{-1} strain-rate region, many 125°C annealed polycarbonate specimens cease to cold-draw and fail by either neck rupturing or crazing. Such specimens are embrittled because of a corresponding decrease in molecular flow and energy to failure.

In neck rupture, failure occurs prior to neck formation but after macroscopic shear zones have propagated to approximately the centre of the specimen. The intersection of the shear bands, which occurs at right-angles, causes a stress concentration[21,75] sufficient to cause a crack to propagate through the planes of the shear bands. Recently, we have observed that this fracture mechanism produces microscopic right-angle steps in certain thermoset resins[23,59,76].

The specimens that deform and fail by crazing alone exhibit large fracture topography initiation regions which often extend up to ~500 μm from the specimen edge. The initiation topography is a porous structure containing 50–100 nm diameter fractured fibrils as illustrated in *Figure 8*. A slow tearing process through the median of the craze produces this topography[51,54,55,57,59,63,74]. Craze and/or crack growth is not inhibited in these specimens by the presence of any cold-drawn oriented material at the craze tip. The absence of the constraints of oriented material in the craze tip region allows the slow-crack growth process to occur.

An overall view of the faster crack-growth fracture topography region of polycarbonate specimens that deformed and failed by crazing is illustrated in *Figure 9a*. A distinct patch pattern is observed in the topography immediately adjacent to the initiation region (*Figure 9b*). This topography is caused by the crack propagating along the craze-matrix boundary interface and jumping irregularly from one boundary to the other[18,33,63,64,74]. Further removed from the initiation region, the topography consists of alternate bands of smooth valleys and rough hills (*Figure 9c*). The bands of rough hills consist of the patch topography which is associated with crack propagation through pre-existing crazes. The patches are, however, on a finer scale than those observed nearer the initiation region in *Figure 9b*. Banded structures have been observed by Jacoby and Cramer[77], Hull and Owen[33] and Ravetti *et al.*[78] in previous studies of polycarbonate fracture topographies.

Bands in the fracture topography has been observed in many other polymers and are generally described in terms of rib markings or striations[33,54,64,77–103]. These bands are

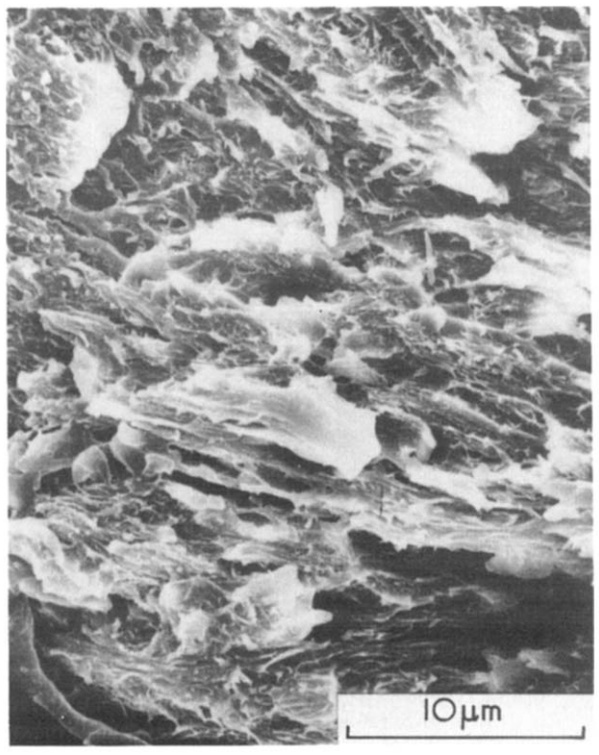

Figure 8 Scanning electron micrograph of fracture topography initiation region of polycarbonate that deformed and failed by crazing under a strain-rate of ~10^{2} min^{-1}

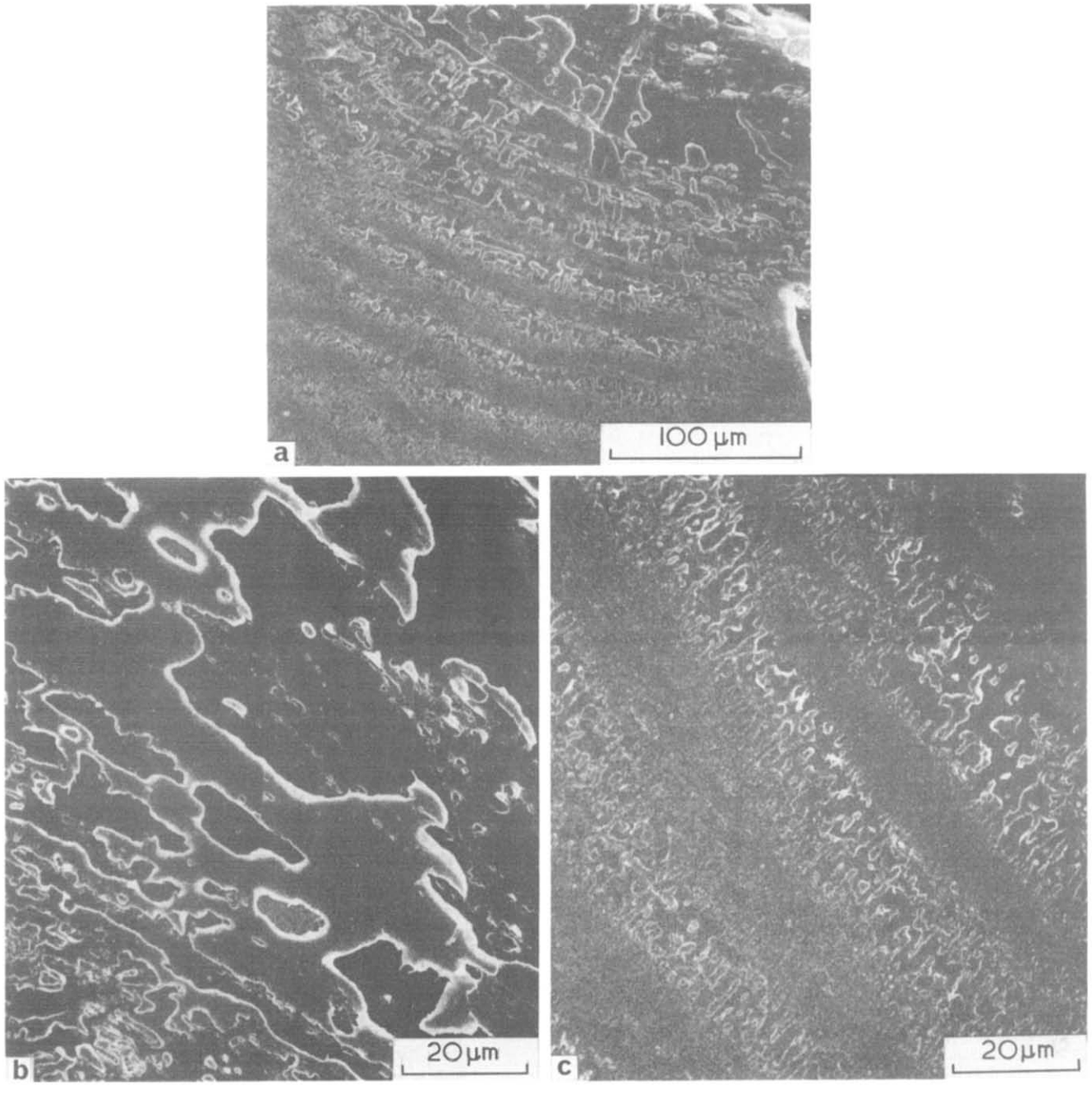

Figure 9 Scanning electron micrographs of the fast crack-growth fracture topography in polycarbonate that deformed and failed by crazing under a strain-rate of $\sim 10^2$ min^{-1} illustrating (a) overall, (b) patch and (c) banded-patch topographies of this region

characteristic of relatively brittle fracture and cover a larger area of the fracture surface, with an accompanying decrease in band spacing, when the molecular weight and/or temperature is decreased and/or the strain-rate is increased. Two different mechanisms have been suggested to explain the banded fracture topographies in polymeric materials: (1) Yoffe[104] has theoretically shown that a crack in an elastic material is expected to accelerate to a limiting velocity and then bifurcate. Andrews[92] notes that branching would be expected to relieve the stress and decelerate the crack. The stress will be restored in a tensile test and, therefore, the processes of crack acceleration followed by bifurcation will be repeated. Craze formation rather than pure crack bifurcation has been suggested to be an intricate part of this slip-stick process in polymers[33,64,100,102]. (2) The banded topographies could also be Wallner lines which are formed at the loci of the intersection of the main-crack front with transverse shock waves released during the fracture processes. Such lines were first observed by Wallner[105] in inorganic glasses. This phenomenon is complex in polymers because any perturbation in the stress caused by shock waves can produce changes in both crack and craze growth, and the growth changes in these two processes may not be the same[33]. In the case of the banded topographies illustrated in *Figure 9*, the mechanism involves a crazing process. However, it is not possible to determine whether the banded topographies arise purely from a slip-stock or a Wallner line mechanism. Kusy and Turner[102] have recently noted that both mechanisms could occur in band formation in poly(methyl methacrylate).

Hence, in the 10^2 min^{-1} strain-rate region, the lower-free-volume, 125°C annealed polycarbonate specimens exhibit evidence of a ductile-brittle transition. These speci-

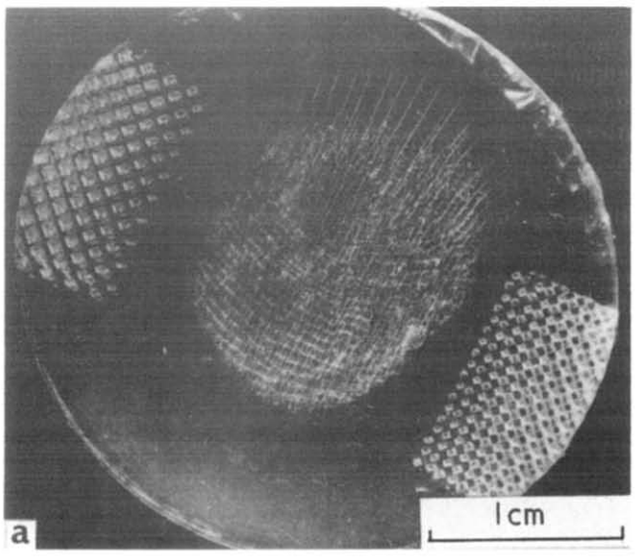

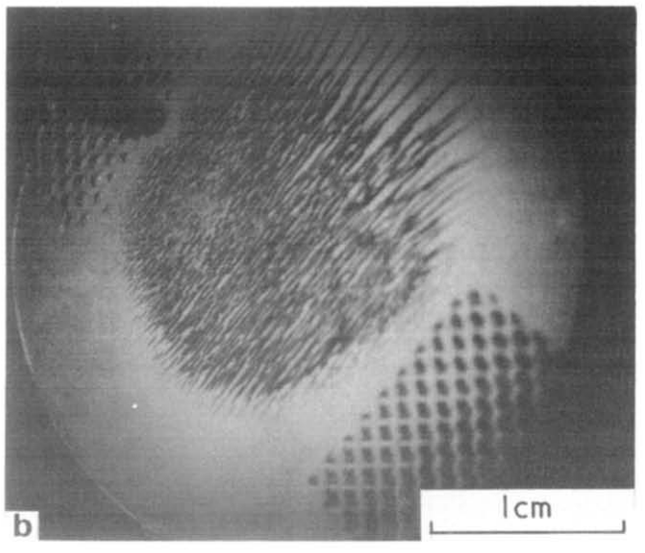

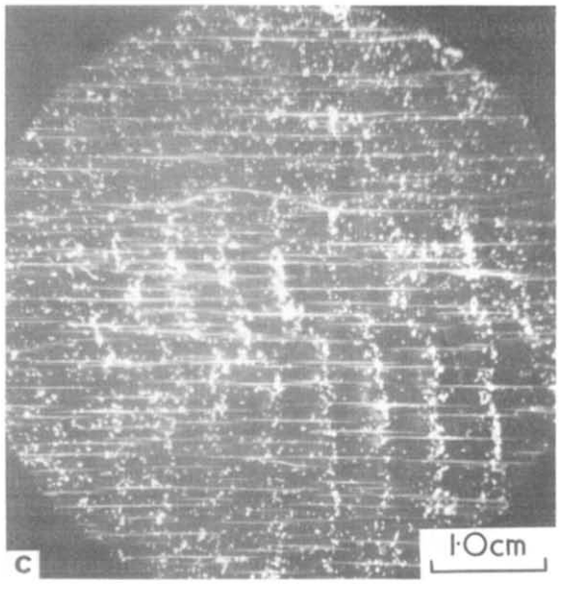

Figure 10 Optical micrographs in (a) reflection, (b) transmission and (c) reflection of crazes that initiated from a thumbprint in polycarbonate

mens embrittle as a result of the cessation of cold-drawing with resultant failure by either neck rupture or crazing with a corresponding decrease in molecular flow and energy to failure. The effect of thermal history and free volume on this ductile-brittle transition have been considered in a previous study[18].

Embrittlement mechanism caused by handling

Caird[8] has documented that handling the surface of polycarbonate followed by exposure to 130°C under stress seriously deteriorates the mechanical properties relative to untouched glasses exposed to the same temperatures and stresses. We investigated the mechanism responsible for this embrittlement by optical and scanning electron microscopy.

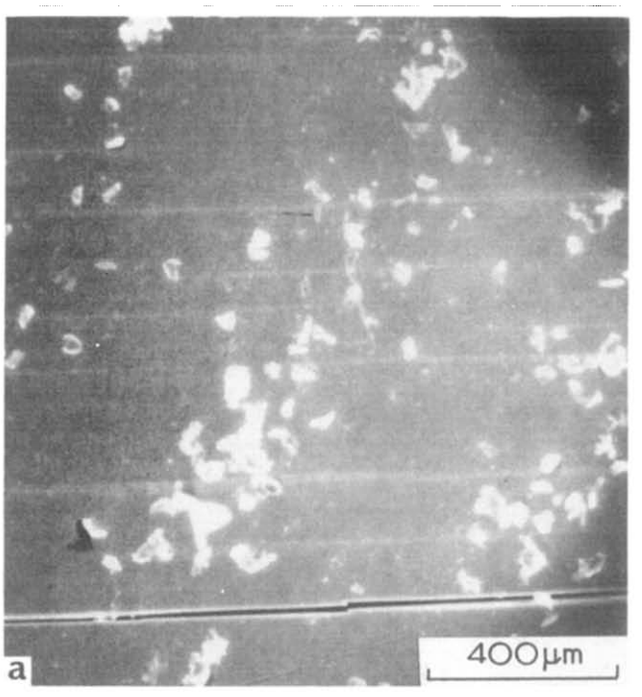

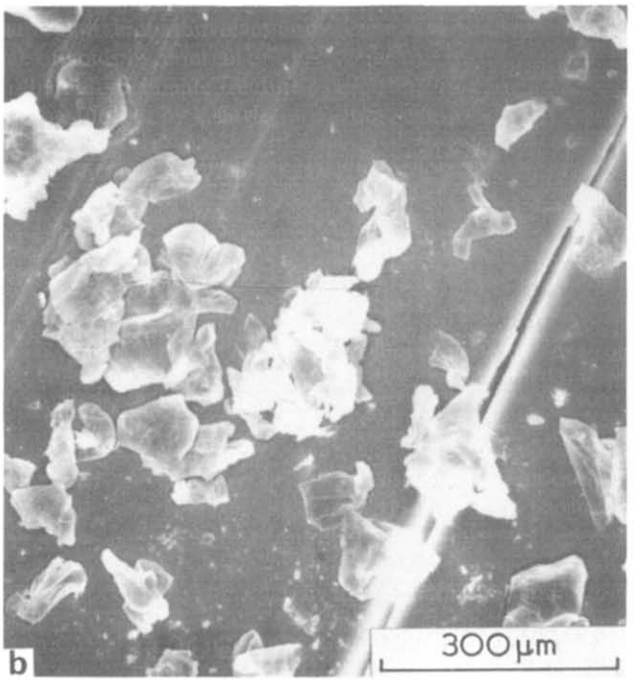

Figure 11 Scanning electron micrographs of crazes in polycarbonate that initiated from islands that had been contacted with fingergrease illustrating (a) overall phenomena and (b) protruding islands

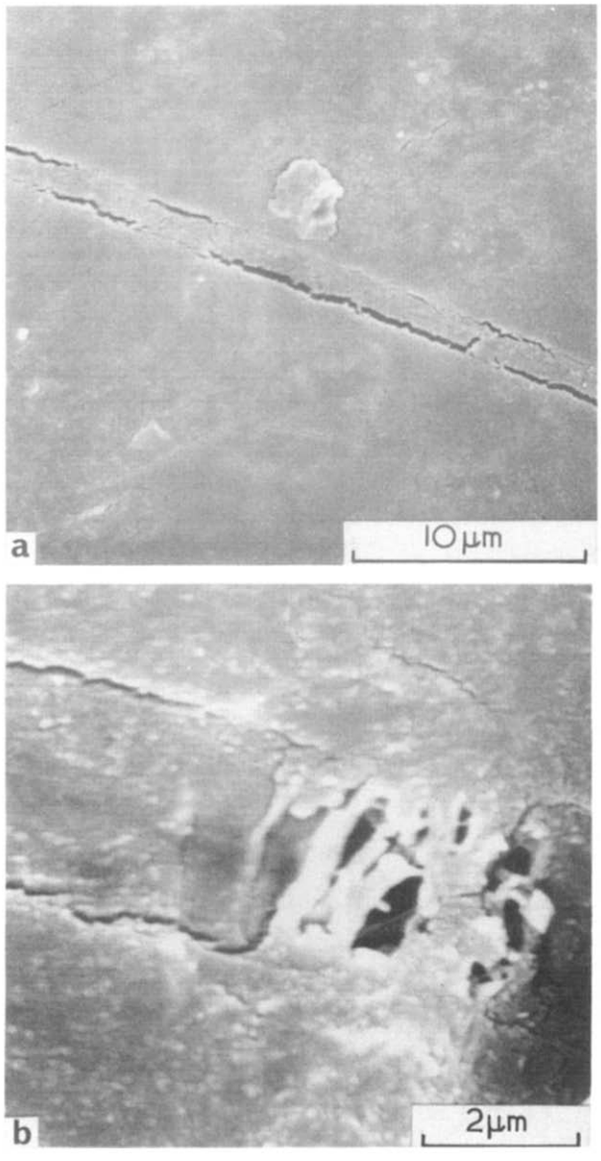

Figure 12 Scanning electron micrographs of surface craze induced by finger-grease in polycarbonate

The optical micrographs in *Figure 10* illustrate crazes that have preferentially grown from a thumbprint after the sample was stressed at 10 MPa for 1h at 130°C. *Figures 10a* and *b* are reflection and transmission optical micrographs respectively of the crazed region. The reflection optical micrograph in *Figure 10c* illustrates the lines of the thumbprint and crazes in more detail. In this latter micrograph the thicker, middle portion of each craze generally coincides with a thumbprint line which suggests that crazes initiated at this line. The thumbprint lines, which consist of ~100 μm sized islands of thumb-grease, and associated cracks and/or crazes are illustrated in more detail in the scanning electron micrograph in *Figure 11a*. *Figure 11b* illustrates protruding areas where thumb-grease has come into contact with the polymer surface; these areas are separated from the surrounding surface, thereby producing a surface microcrack ~100 μm in length. These cracks act as stress concentrators for craze initiation and growth which leads to premature failure prior to the development of significant flow via shear-band deformation. The parallel lines in *Figure 11b* are well-developed cracks and/or crazes that have initiated from the ~100 μm microcracks that surround the plasticized islands. The surface crazes often appear as linear surface depressions with parallel cracks along their edges in scanning electron microscopy (*Figure 12a*). Evidence of the fibrillar craze structure was observed in isolated regions in these micrographs as illustrated in *Figure 12b*.

From the preceding observations, the following mechanism is suggested by which finger-grease causes surface microcracking. The regions of polycarbonate that have come into contact with finger-grease are plasticized and, therefore, fabrication stresses in such regions relax at a faster rate than those in the unplasticized surroundings. These islands separate from their surroundings and rise above the general surface contour when the fabrication stresses and orientation are parallel to the polymer surface. The inhomogeneous distribution of the plasticizing agent is a significant factor in this particular solvent-crazing mechanism. However, smearing finger-grease to produce a continuous surface grease layer still produces general microcracking, following stress and temperature exposure, as a result of a general relaxation of fabrication stresses. These microcracks which are illustrated in *Figure 13* are, however, < 10 μm in length which is a factor of 10 smaller than those produced from the plasticized islands.

These studies produced no evidence that solvent-induced surface crystallization plays any role in the craze initiation and growth processes.

Deformation processes in polycarbonate films strained directly in the electron microscope

Polycarbonate films ~1 μm thick, were strained directly in the electron microscope. These films deformed and failed by crazing as illustrated in the transmission electron micrographs in *Figure 14*. Crazes initiate as thinned regions in these films rather than by void formation. This thinning process has been previously reported in thin polycarbonate

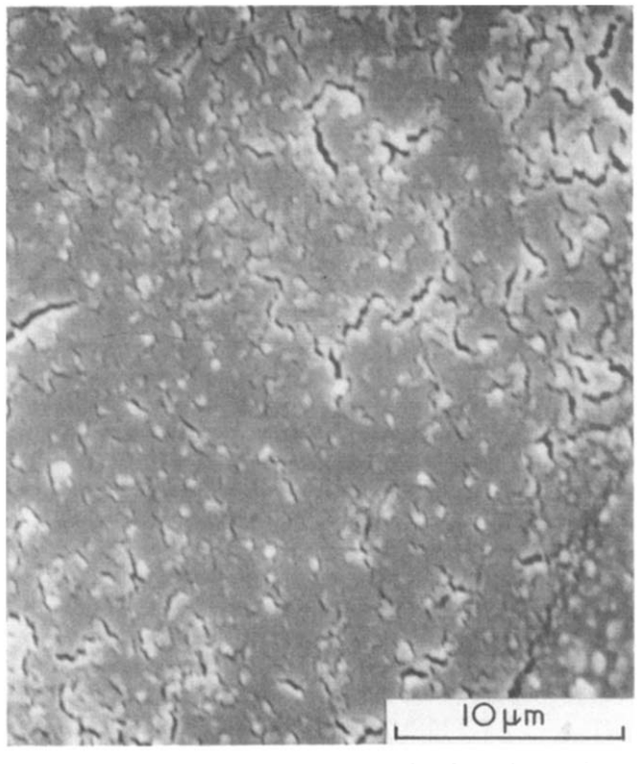

Figure 13 Scanning electron micrograph of surface microcracks in polycarbonate induced by a layer of finger-grease

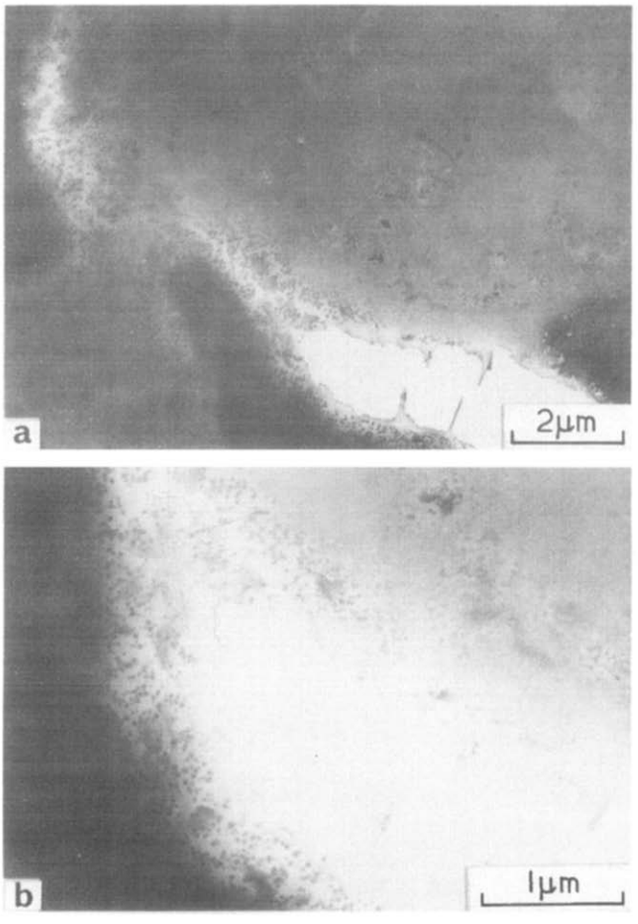

Figure 14 Bright-field transmission electron micrographs of a craze in a strained polycarbonate thin film illustrating (a) overall craze and surroundings and (b) craze structure

films by Wyzgoski and Yeh[4] and Thomas and Israel[5] and is attributed to the lateral contraction of the film during deformation. Voids and fibrils develop in the later stages of growth in these regions; the remnants of such fractured fibrils are evident in *Figure 14*.

In the thinned regions and the craze fibrils in the micrographs in *Figure 14*, dark, ~10 nm sized nodular regions are evident. These regions are evidently less susceptible to deformation and do not break-up and become thinner during the flow processes but simply move past one another. These less-deformable, ~10 nm sized nodular regions are illustrated in more detail in the craze-crack tip region in the bright-field transmission electron micrograph in *Figure 15*. Such nodular regions appear dark in bright-field transmission because they are thicker than their surroundings. It is uncertain whether such regions are (a) precrystalline nodular structures, (b) less-deformable regions produced by electron-beam damage or (c) thicker regions produced during the solvent evaporation processes. Certainly precrystalline and/or crystalline entities can form during film fabrication from solution or grow below the bulk T_g in thin films or on free surfaces where mobility restrictions are less severe than in the bulk[18]. Hence, if these less-deformable regions are a consequence of surface crystallization processes in polycarbonate, such regions could also be present on the surfaces of bulk specimens and play a role in the bulk craze initiation processes.

CONCLUSIONS

The flow processes and toughness of glassy polycarbonate in tension are controlled by the ease of shear-band deformation and the resultant strain-hardening characteristics of the cold-drawn material, together with the characteristics of surface crazes which form prior to macroscopic necking. The geometry and physical structure of the surface crazes together with the crack resistance of the oriented polymer can directly control at what stage of deformation fracture occurs, and, hence, toughness of the polymer. The characteristics of these surface crazes varied as a function of strain-rate in 1 mm thick polycarbonate specimens deformed in tension at room temperature. In the 10^{-2}–10^{+2} min^{-1} strain-rate region, the polycarbonate specimens deformed predominantly by shear-band deformation and cold drawing. However, surface crazes that form prior to macroscopic necking and cold-drawing serve as sites for ultimate fracture. In the 10^{-2}–1 min^{-1} strain-rate region, the crazes grow to ~5–10 μm in length prior to macroscopic shear-band deformation. Subsequent cold-drawing leads to the growth of these craze sites by plastic tearing. In the 1–10^2 min^{-1} strain-rate region, larger surface crazes up to ~100 μm in length develop prior to macroscopic shear-band deformation. These crazes, however, do not significantly grow in area prior to catastrophic crack propagation through the oriented, cold-drawn material. In the ~10^2 min^{-1} strain-rate region, specimens with low free-volumes, as a result of annealing at 125°C, ceased to cold-draw and deformed and failed either by crazing or by a neck rupture process. Such specimens are embrittled because of a corresponding decrease in molecular flow and energy to failure.

Surface crazing is enhanced in polycarbonate by environmental factors such as handling. The regions of the polycarbonate surface that have come into contact with fingergrease are plasticized, and fabrication stresses in such regions relax near T_g at a faster rate than those in the unplasticized surroundings. The plasticized, relaxed regions separate from their surroundings producing microcracks which serve as sites for craze initiation and growth, and possible embrittlement of the polymer.

Crazes initiated and propagated in thin polycarbonate films that were deformed directly in the electron microscope. Nodular regions, ~10 nm in size, which did not break-up

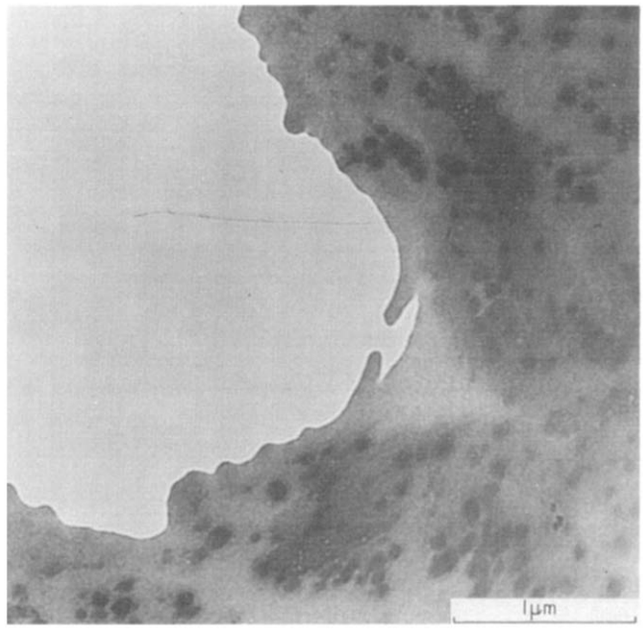

Figure 15 Bright-field transmission electron micrograph of craze-crack tip region in strained polycarbonate thin film

during the craze flow processes were observed in these films.

ACKNOWLEDGEMENTS

The authors wish to acknowledge Lt. Col. Richard Haffner and Dr. Donald Ulrich (AFOSR), and Drs. Donald P. Ames and Clarence J. Wolf (MDRL, St. Louis) for their support and encouragement of this work.

REFERENCES

1 Spurr, O. K., Jr. and Neigisch, W. D., *J. Appl. Polym. Sci.* 1962, **6**, 585
2 Miller, G. W., Visser, S. A. D., and Morecroft, A. S., *Polym. Eng. Sci.* 1971, **11**, 73
3 Kambour, R. P. *Macromol. Rev.* 1973, **7**, 1
4 Wyzgoski, M. G. and Yeh, G. S. Y., *J. Macromol. Sci. (B)* 1974, **10(3)**, 441 and 647
5 Thomas, E. L. and Israel, S. J., *J. Mater. Sci.* 1975, **10**, 1603
6 Brown, N. and Imai, Y., *J. Appl. Phys.* 1975, **46**, 4130
7 Ohishi, F., Nakamura, S., Koyama, D., Minabe, K., Fujisawa, Y., and Tsuruga, Y., *J. Appl. Polym. Sci.* 1976, **20**, 79
8 Caird, D. W., Proc. of Air Force Conference on Aerospace Transparent Materials and Enclosures, AFML-TR-76-54 (1976) p 367
9 Peilstocker, G., *Kunststoffe* 1961, **51**, 509
10 Peilstocker, G., *Brit. Plastics* 1962, **35**, 365
11 Golden, J. H., Hammant, B. L., and Hazell, E. A. *J. Appl. Polym. Sci.* 1967, **11**, 1571
12 LeGrand, D. G., *J. Appl. Polym. Sci.* 1969, **13**, 2129
13 LeGrand, D. G., *J. Appl. Polym. Sci.* 1972, **16**, 1367
14 Robertson, R. E. and Joynson, C. W., *J. Appl. Polym. Sci.* 1972, **16**, 733
15 Allen, G., Morley, D. C. W., and Williams, T., *J. Mater. Sci.* 1973, **8**, 1449
16 Morgan, R. J. and O'Neal, J. E., *Polym. Plast. Tech. and Eng.* 1975, **5(2)**, 173
17 Adam, G.A., Cross, A., and Haward, R. N., *J. Mater. Sci.* 1975, **10**, 1582
18 Morgan, R. J. and O'Neal, J. E., *J. Polym. Sci. (Polym. Phys. Edn)* 1976, **14**, 1053
19 Morgan, R. J. and O'Neal, J. E. in *Toughness and Brittleness of Plastics, Advances in Chemistry Series 154*, Eds. Deanin, R. D. and Grugnola, A. M., (ACS, Washington, D. C., 1976) Ch 2
20 Morgan, R. J., Proc. of Air Force Conference on Aerospace Transparent Materials and Enclosures, AFML-TR-76-54 (1976) p 349
21 Mills, N. J. *J. Mater. Sci.* 1976, **11**, 363
22 Yee, A. F., *J. Mater. Sci.* 1977, **12**, 757
23 Morgan, R. J. and O'Neal, J. E., *Org. Plast. Coat. Preprints (ACS)* 1977, **37(2)**,480
24 Renninger, A. L., Wicks, G. G., and Uhlmann, D. R., *J. Polym. Sci. (Polym. Phys. Edn)* 1975, **13**, 1247
25 Wignall, G. D. and Longman, G. W. *J. Macromol. Sci. (B)* 1976, **12(1)**, 99
26 Frank, W., Goddar, H., and Stuart, H. A. *J. Polym. Sci. (B)* 1967, **5**, 711
27 Carr, S. H., Geil, P. H. and Baer, E., *J. Macromol. Sci. (B)* 1968, **2(1)**, 13
28 Siegmann, A. and Geil, P. H. *J. Macromol. Sci. (B)* 1970, **4(2)**, 239 and 273
29 Neki, K. and Geil, P. H. *J. Macromol. Sci. (B)* 1973, **8(1–2)**, 295
30 Wyzgoski, M. G. and Yeh, G. S. Y., *Int. J. Polymeric. Mater.* 1974, **3**, 149
31 Geil, P. H., *J. Macromol. Sci. (B)* 1976, **12(2)**, 173
32 Takano, M. and Nielson, L. E. *J. Appl. Polym. Sci.* 1976, **20**, 2193
33 Hull, D. and Owen, T. W., *J. Polym. Sci. (Polym. Phys. Edn)* 1973, **11**, 2039
34 Parvin, M. and Williams, J. G., *J. Mater. Sci.* 1975, **10**, 1833
35 Kambour, R. P. and Miller, S., *J. Mater. Sci.* 1976, **11**, 823
36 Ishikawa, M., Narisawa, I., and Ogawa, H., *J. Polym. Sci. (Polym. Phys. Edn.)* 1977, **15**, 1791
37 Kambour, R. P. and Miller, S., *J. Mater. Sci.* 1977, **12**, 2281
38 Fraser, R. A. W. and Ward, I. M., *J. Mater. Sci.* 1977, **12**, 459
39 Kastelic, J. R. and Baer, E., *J. Macromol. Sci. (B)* 1973, **7(4)**, 679
40 Cornes, P. L., Smith, K., and Haward, R. N. *J. Polym. Sci. (Polym. Phys. Edn)* 1977, **15**, 955
41 Moore, W. R. and Sheldon, R. P. *Polymer* 1961, **2**, 315
42 Kambour, R. P., Karasz, F. E., and Duane, J. M. *J. Polym. Sci. (A)*, 1966, **2, 4**, 327
43 Mercier, J. P., Groeninckx, G., and Lesne, M., *J. Polym. Sci. C*, 1967, **16**, 2059
44 Titow, W. V., Braden, M., Currell, B. R. and Loneragan, R. J. *J. Appl. Polym. Sci.* 1974, **18**, 867
45 Gallez, F., Legras, R., and Mercier, J. P. *J. Polym. Sci. (Polym. Phys. Edn.)* 1976, **14**, 1367
46 Kambour, R. P. , *Polymer* 1964, **5**, 143
47 Kambour, R. P. and Holik, A. S., *J. Polym. Sci. (A)* 1969, **2, 7**, 1393
48 Kambour, R. P. and Russell, R. R., *Polymer* 1971, **12**, 237
49 Klement, J. J. and Geil, P. H. *J. Macromol. Sci. (B)*, 1972, **6(1)**, 31
50 Morgan, R. J. and O'Neal, J. E., *J. Mater. Sci.* 1977, **12**, 1338
51 Morgan, R. J. and O'Neal, J. E., *J. Mater. Sci.* 1977, **12**, 1966
52 Morgan, R. J. and O'Neal, J. E., in *Chemistry and Properties of Crosslinked Polymers*, E. Labana, S. S. (Academic Press, 1977) p 289
53 Owen, M. J. and Rose, R. G. *J. Mater. Sci.* 1975, **10**, 1711
54 Morgan, R. J. and O'Neal, J. E., *J. Macromol. Sci. (B)*, 1978, **15(1)**, 139
55 Murray, J. and Hull, D., *J. Polym. Sci. (A)*, 1970, **2, 8**, 1521
56 Doyle, M. J., *J. Polym. Sci. (Polym. Phys. Edn.)* 1975, **13**, 127
57 Doyle, M. J., *J. Mater. Sci.* 1975, **10**, 300
58 Hoare, J. and Hull, D., *J. Mater. Sci.* 1975, **10**, 1861
59 Morgan, R. J. and O'Neal, J. E., *Polym. Plast. Tech. and Eng.* 1978, **10(1)**, 49
60 Cornes, P. L. and Haward, R. N. *Polymer* 1974, **15**, 149
61 Tormala, P., Lehtinen, S., and Lindberg, J. J. *J. Mater. Sci.* 1976, **11**, 1764
62 Smith, K. and Haward, R. N. *Polymer* 1977, **18**, 746
63 Murray, J. and Hull, D., *Polymer* 1969, **10**, 451
64 Murray, J. and Hull, D., *J. Polym. Sci. A-2*, 1970, 8, 583
65 Cottrell, A. H., in *Fracture*, Eds. Averbach, B. L., Felbeck, D. K., Hahn, G. T. and Thomas, D. A. (Wiley, 1959) p 20
66 Rogers, H., *Trans. Met. Soc. AIME* 1960, **218**, 498
67 Low Jun, J. R., *Eng. Fract. Mech.* 1968, 1, 47
68 Hertzberg, R. W. and Manson, J. A. *J. Mater. Sci.* 1973, **8**, 1554
69 Skibo, M. D., Hertzberg, R. W. and Manson, J. A. *J. Mater. Sci.* 1976, **11**, 479
70 Skibo, M. D., Hertzberg, R. W., Manson, J. A., and Kim, S. L. *J. Mater. Sci.* 1977, **12**, 531
71 Rabinowitz, S. and Beardmore, P., in *Critical Reviews in Macromolecular Science* (Chem. Rubber Company, Cleveland, 1972), Vol. 1, p 1
72 Rehage, G. and Goldbach, G., *Angew. Macromol. Chem.* 1967, **1**, 125
73 Haward, R. N., Murphy, B. M., and White, E. F. T., *Fracture*, Proc. 2nd Int. Conf. Fracture, Brighton (Chapman and Hall, London, 1969), p 579
74 Beahan, P., Bevis, M., and Hull, D., *J. Mater. Sci.* 1972, **8**, 162
75 Hull, D., *Acta Met.* 1960, **8**, 11
76 Morgan, R. J., O'Neal, J. E. and Miller, D. B. *J. Mater. Sci.* (in press)
77 Jacoby, G. and Cramer, C., *Rheol. Acta*, 1968, 7, 23
78 Ravetti, R., Gerberich, W. W., and Hutchinson, T. E. *J. Mater. Sci.* 1975, **10**, 1441
79 Rexer, E., *Z. Tech. Phys.* 1939, **20**, 97
80 Kies, J. A., Sullivan, A. M., and Irwin, G. R., *J. Appl. Phys.* 1950, **21**, 716
81 Hsiao, C. C. and Sauer, J. A., *J. Appl. Phys.* 1950, **21**, 1071
82 Cheatham, R. G. and Dietz, A. G. H. *Mod. Plast.* 1951, **29**, No. 1, 113
83 Zanderman, F., Publs, Scient. Tech. Minist. Air, Paris, No. 291 (1954) Ch. IV
84 Leeuwerik, J. and Schwarzl, F., *Plastica* 1955, **8**, 474
85 Smith, D. C., *Nature* 1958, **182**, 132
86 Newman, S. B. and Wolock, I., *J. Appl. Phys.* 1958, **29**, 49
87 Andrews, E. H., *J. Appl. Phys.* 1959, **30**, 740
88 Benbow, J. *J. Proc. Phys. Soc.* 1961, **78**, 970

89 Wolock, I. and Newman, S. B., in *Fracture Processes in Polymeric Solids,* Ed. Rosen, B. (Interscience, 1964) Ch. IIc
90 Broutman, L. J. and McGarry, F. J., *J. Appl. Polym. Sci.* 1965, **9**, 589
91 Cottrell, B., *Appl. Mater. Res.* 1965, **4**, 227
92 Andrews, E. H., *Fracture in Polymers* (Elsevier, New York, 1968)
93 Murray, J. and Hull, D., *J. Polym. Sci. (B)* 1970, **8**, 159
94 Hull, D., *J. Mater. Sci.* 1970, **5**, 357
95 Doyle, M. J., Maranci, A., Orowan, E., and Stork, S. T. *Proc. Roy. Soc. (London)* 1972, **A239**, 137
96 Moskowitz, H. D. and Turner, D. T. *J. Mater. Sci.* 1974, **9**, 861
97 Doyle, M. J., *J. Mater. Sci.* 1975, **10**, 159
98 Doll, W., *J. Mater. Sci.* 1975, **10**, 935
99 Kusy, R. P., *J. Mater. Sci.* 1976, **11**, 1381
100 Kusy, R. P., Lee, H. B. and Turner, D. T. *J. Mater. Sci.* 1976, **11**, 118
101 Friederich, K., *J. Mater. Sci.* 1977, **12**, 640
102 Kusy, R. P. and Turner, D. T. *Polymer* 1977, **18**, 391
103 Kusy, R. P., Lee, H. B. and Turner, D. T. *J. Mater. Sci.* 1977, **12**, 1694
104 Yoffe, E. H. *Phil. Mag.* 1951, **42**, 739
105 Wallner, H., *Z. Phys.* 1939, **114**, 368